

## A Quantum Dot Conjugated Sugar Ball and Its Cellular Uptake. On the Size Effects of Endocytosis in the Subviral Region

Fumio Osaki, Takuya Kanamori, Shinsuke Sando, Takashi Sera, and Yasuhiro Aoyama\*

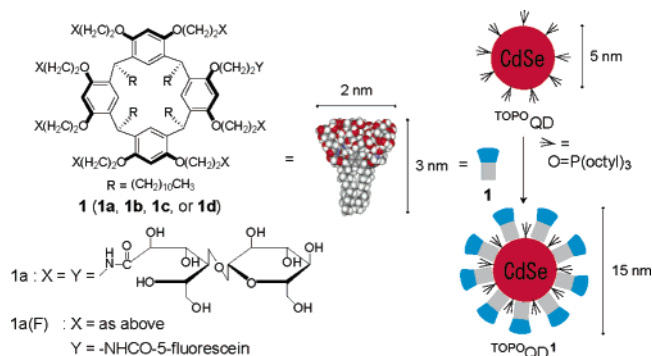
Department of Synthetic Chemistry and Biological Chemistry, Graduate School of Engineering, Kyoto University, Katsura, Nishikyo-ku, Kyoto 615-8510, Japan

Received March 2, 2004; E-mail: aoyamay@sbchem.kyoto-u.ac.jp

Endocytosis is the drinking activity of eukaryotic cells, which thereby ingest a part of their plasma membrane continually to form endocytic vesicles ( $\leq 100$  nm), into which external objects are swallowed. This suggests that endocytosis-susceptible guest particles have an upper size limit of  $\sim 100$  nm. The size of many viruses meaningfully falls in the range of 20–100 nm. We recently reported an artificial glycoviral gene delivery system,<sup>1</sup> where only monomeric “glycoviruses” ( $\sim 50$  nm) possess substantial endocytosis-mediated transfection activities.<sup>1</sup> This is in agreement with the 100-nm size limit. A question then arises which is essential when designing artificial molecular (drug, gene, probe, etc.) delivery machines:<sup>2</sup> is there any lower size limit or do smaller particles undergo readier endocytosis? Actually, little is known about the size effects of endocytosis in the subviral size region ( $\leq 50$  nm), primarily because of the lack of appropriate size markers. We notice here the utility of quantum dots (QDs) in this context. QDs are inorganic semiconductor nanocrystals (2–6 nm), whose unique fluorescence properties (strong, sharp, stable, and size-tunable emission) make them attractive biolabels<sup>3–6</sup> when they are suitably functionalized with biomolecules such as protein and DNA. The present work is concerned about saccharide coating of QD.<sup>6</sup> We report here that the resulting QD-conjugated sugar ball serves as a 15-nm endosome marker and reveals a remarkable size effect in endocytosis.

The lipophilic CdSe QD coated with trioctylphosphine oxide (TOPOQD in Scheme 1;  $d = 5$  nm for the core QD (Figure S1) and

**Scheme 1.** Formation of TOPOQD<sup>1</sup> upon Coating of TOPOQD with Glycocluster Amphiphile **1**; the Terminal Saccharide Moieties in **1b**, **1c**, and **1d** Are  $\beta$ -Galactoside,  $\alpha$ -Glucoside, and  $\alpha$ -Maltotetraoside, Respectively, in Place of  $\beta$ -Glucoside in **1a**



$\lambda_{em} = 622$  nm)<sup>7,8</sup> is completely insoluble in water but is extracted thereto when a chloroform solution of the former (2.3  $\mu$ M, 1.5 mL) is vigorously stirred (vortexed) for 1 h at room temperature with an aqueous solution of cone-shaped amphiphile **1**<sup>9</sup> (1.4 mM, 1.5 mL) having four long alkyl (R = (CH<sub>2</sub>)<sub>10</sub>CH<sub>3</sub>) chains and eight saccharide moieties (cellobiose- (**1a**), lactose- (**1b**), maltose- (**1c**), or maltoheptaose-derived (**1d**)) on the opposite sides of the calix[4]resorcinarene macrocycle (Scheme 1). The water-solubilized QD

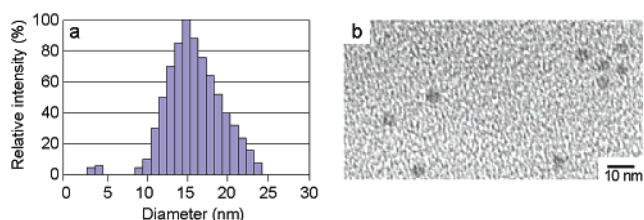
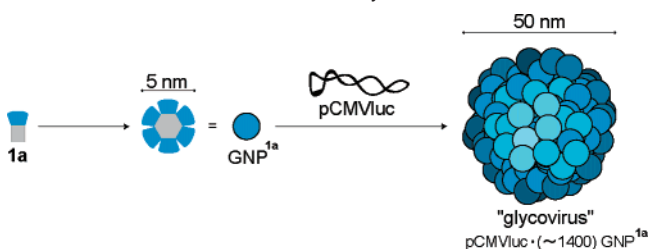


**Figure 1.** DLS size distribution profile for TOPOQD<sup>1c</sup> (a; in reference to intensity of scattered light which theoretically shows a  $10^6$  dependence on the size of particle; particle of  $\sim 4$  nm size is GNP<sup>1c</sup>) and TEM image for TOPOQD<sup>1a</sup> (b, no staining) as extracted in water containing **1c** or **1a**.

**Scheme 2.** Formation of GNP and Glycovirus from **1a**



species (TOPOQD<sup>1</sup>; **1** = **1a**, **1b**, **1c**, or **1d**) thus extracted ( $\sim 10\%$  based on TOPOQD used) fluoresces at  $\lambda_{em} = 620$  nm (Figure S2),<sup>8</sup> appears as a 15-nm sized particle in DLS (Figure 1a, intensity-weighted), manifests itself in TEM (Figure 1b, no staining), and is stable when amphiphile **1** is present in excess.

The four alkyl chains of the present glycocluster amphiphiles provide a potent site of hydrophobic association. They thus form  $\sim 5$  nm sized micellar glycocluster nanoparticles (GNPs) having an aggregation number of 6 (Scheme 2)<sup>1,9</sup> and are also readily immobilized on hydrophobic platforms such as hydrophobized sensor chip of SPR.<sup>9</sup> This leaves little doubt that, upon extraction, the TOPO-coated QD (TOPOQD) undergoes further coating with amphiphile **1** (TOPOQD<sup>1</sup> in Scheme 1), the alkyl tails of which are embedded in the hydrophobic forest of TOPOQD with the saccharide moieties being exposed to bulk water.<sup>10</sup> The observed DLS size of 15 nm is in good agreement with this structure, judging from the molecular dimensions of TOPO and **1** (Scheme 1). The core QD retains the original size of 5 nm (Figure 1b); there is no extraction-induced or extraction-responsible fusion/aggregation thereof.

We then examine the cell affinities by fluorescence microscopy (Figure 2). When treated with HeLa cells (HeLa(F) cells) whose endosomes have been specifically labeled by green fluorescence protein GFP (a, excitation (ex) at 470–490 nm and detection (de) at 515–550 nm),<sup>1</sup> red-fluorescing (ex at 520–550 nm and de at  $> 580$  nm) TOPOQD<sup>1</sup> in a dilute solution (0.5 nM) readily invades the cells to give red spots (b), which, upon computer overlap with micrograph a, turn yellow (c) as a result of merge of red and green colors. This indicates that the QD-conjugated 15-nm sugar ball

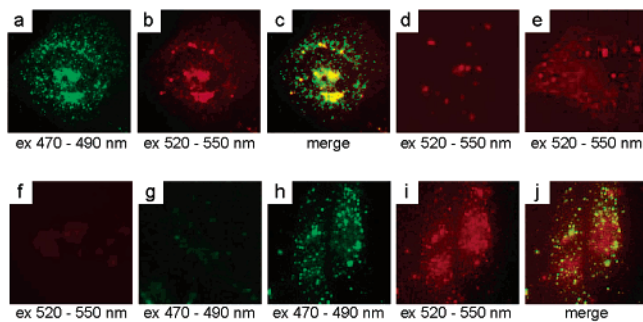


**Figure 2.** Fluorescence micrographs of HeLa cells (either labeled (HeLa(F)) or unlabeled (HeLa) with GFP at endosomes) treated with a DMEM medium containing the following additives at 37 °C for 15 min, followed by washing of the cells with PBS. Cells used and additives are (a and b) HeLa(F) and  $\text{TOPOQD}^{1a}$  (0.5 nM) with excess **1a** (3  $\mu\text{M}$ ;  $[\text{GNP}^{1a}] = 0.5 \mu\text{M}$ ), (d) HeLa and plasmid-labeled glycovirus pCMVluc(F) $\cdot(\sim 1400)\text{GNP}^{1a}$  (0.5 nM) with excess **1a** (3  $\mu\text{M}$ ;  $[\text{GNP}^{1a}] = 0.5 \mu\text{M}$ ), (e) HeLa and  $\text{TOPOQD}^{1a}$  (0.5 nM) with excess **1a** (3  $\mu\text{M}$ ;  $[\text{GNP}^{1a}] = 0.5 \mu\text{M}$ ), (f) HeLa and  $\text{TOPOQD}^{1a}$  (0.5 nM) and plasmid-unlabeled glycovirus pCMVluc $\cdot(\sim 1400)\text{GNP}^{1a}$  with excess **1a** (3  $\mu\text{M}$ ;  $[\text{GNP}^{1a}] = 0.5 \mu\text{M}$ ), (g) HeLa and **1a**(F) (10  $\mu\text{M}$ ;  $[\text{GNP}^{1a(F)}] = 2 \mu\text{M}$ ), and (h and i)  $\text{TOPOQD}^{1a(F)}$  (0.5 nM) with excess **1a**(F) (3  $\mu\text{M}$ ;  $[\text{GNP}^{1a(F)}] = 0.5 \mu\text{M}$ ). Excitation wavelengths are as indicated. Panels c and j: computer overlap of a and b and h and i, respectively.

$\text{TOPOQD}^1$  is taken up by the cells via endocytosis,<sup>11</sup> thereby being first trapped in the endocytic vesicles and then transferred into endosomes. In the same manner, we previously demonstrated<sup>1</sup> the facile endocytic uptake of a 50-nm sized artificial “glycovirus” pCMVluc(F) $\cdot(\sim 1400)\text{GNP}^{1a}$  (d), in which 7040 base-pair plasmid DNA pCMVluc with specific rhodamine-labeling at the G moieties (“(F)” denotes fluorescence labeling) is stoichiometrically coated with  $\sim 1400$  micellar particles (GNPs) of amphiphile **1a** (Scheme 2). Interestingly, there is a big difference in the activities of the two particles. The otherwise facile incorporation of  $\text{TOPOQD}^{1a}$  (e) is completely inhibited (f) by the presence of an equimolar amount (0.5 nM) of the glycovirus pCMVluc $\cdot(\sim 1400)\text{GNP}^{1a}$  containing an intact plasmid without fluorescence labeling. Thus, the “competition” between  $\text{TOPOQD}^{1a}$  (15 nm) and pCMVluc $\cdot(\sim 1400)\text{GNP}^{1a}$  (50 nm) is remarkably in favor of the latter.

To step further toward the size effects, we need to know the endocytosis activity of the micellar homoaggregate of amphiphile **1a**, referred to as  $\text{GNP}^{1a}$  above (Scheme 2), which exists in a large excess in a solution of  $\text{TOPOQD}^{1a}$  or pCMVluc $\cdot(\sim 1400)\text{GNP}^{1a}$ . Fluorescein-labeled probe **1a**(F) (Scheme 1, Supporting Information for the preparation) forms 5-nm sized micellar particles ( $\text{GNP}^{1a(F)}$ ) and is capable of extracting the QD to form  $\text{TOPOQD}^{1a(F)}$  of a 15-nm DLS size in a similar manner as parent **1a**. Fluorescence monitoring of HeLa cells (no endosome labeling) incubated in a 10  $\mu\text{M}$  solution of green-fluorescent probe **1a**(F) alone ( $[\text{GNP}^{1a(F)}] \cong 2 \mu\text{M}$ ) reveals that there is very little fluorescence development in the cells even at the highest sensitivity (g). When incubated in a solution of  $\text{TOPOQD}^{1a(F)}$  (0.5 nM) and excess **1a**(F) (3  $\mu\text{M}$  or  $[\text{GNP}^{1a(F)}] \cong 0.5 \mu\text{M}$ ), the cells take up the former to give red-fluorescing (ex at 520–550 nm) endosomes (i), which are also green-fluorescent upon excitation at 470–490 nm (h) and give rise to yellow color upon color merge (j). These results indicate that the otherwise endocytosis-inactive molecular or micellar probe **1a**(F)/ $\text{GNP}^{1a(F)}$  in a  $\mu\text{M}$  region can invade the cells when conjugated with QD even in the nM range and that the resulting complex  $\text{TOPOQD}^{1a(F)}$  in the endosomes exists as such, i.e., without undergoing dissociation/decomplexation into components QD (red) and **1a**(F) (green).

To summarize, surface coverage of lipophilic  $\text{TOPOQD}$  with the quadruple-chain octa(saccharide) amphiphile **1** affords a novel QD-conjugated sugar ball (15 nm), which marks endosomes much more and much less efficiently than the micellar homoaggregate of the amphiphile (GNP, 5 nm) and the virus-like DNA–GNP conjugate (50 nm), respectively. Although their different nature precludes any rigorous comparison, the dramatic difference in the activities of the three nanoparticles which are commonly **1a**-coated and hence neutral and highly hydrophilic strongly suggests that endocytosis is highly size-dependent ( $50 \gg 15 \gg 5$ ). We also note that glycovirus aggregates ( $> 100$  nm) are incorporated only slightly in the cells.<sup>1</sup> These results may be combined to suggest an optimal size at around 50 nm. The size of potential guests of endocytosis such as viruses and lipid-carrying proteins indeed falls in this range.<sup>12</sup> Thus, the size complementarity that governs molecular recognition in small host–guest systems seems to play key roles also in the encapsulation of nanometric guest particles by the endocytic vesicles as a macromolecular host. In designing artificial molecular delivery systems, size control at the viral size would be of an utmost importance.

**Acknowledgment.** We thank T. Nakai. This work was supported by RFTF of JSPS and by Grant-in-Aids for Scientific Research (No. 13490021) and for 21st COE on Kyoto University Alliance for Chemistry from the Japanese Government.

**Supporting Information Available:** Preparation of compound **1a**(F), Figure S1 (TEM of  $\text{TOPOQD}$ ), and Figure S2 (fluorescence spectrum of  $\text{TOPOQD}^{1b}$ ). This material is available free of charge via the Internet at <http://pubs.acs.org>.

## References

- (1) Nakai, T.; Kanamori, T.; Sando, S.; Aoyama, Y. *J. Am. Chem. Soc.* **2003**, *125*, 8465–8475.
- (2) (a) Blessing, T.; Remy, J.-S.; Behr, J.-P. *J. Am. Chem. Soc.* **1998**, *120*, 8519–8520. (b) *Self-assembling Complexes for Gene Delivery. From Laboratory to Clinical Trial*; Kabanov, A. V., Felgner, P. L., Seymour, L. W., Eds.; Wiley: Chichester, 1998.
- (3) (a) Bruchez, M., Jr.; Moronne, M.; Gin, P.; Weiss, S.; Alivisatos, A. P. *Science* **1998**, *281*, 2013–2016. (b) Chan, W. C.; Nie, S. *Science* **1998**, *281*, 2016–2018.
- (4) (a) Niemeyer, C. M. *Angew. Chem., Int. Ed.* **2001**, *40*, 4128–4158. (b) Chan, W. C. W.; Maxwell, D. J.; Gao, X.; Bailey, R. E.; Han, M.; Nie, S. *Curr. Opin. Biotechnol.* **2002**, *13*, 40–46.
- (5) (a) Han, M.; Gao, X.; Su, J. Z.; Nie, S. *Nat. Biotechnol.* **2001**, *19*, 631–635. (b) Dubertret, B.; Skourides, P.; Norris, D. J.; Noireaux, V.; Brivanlou, A. H.; Libchaber, A. *Science* **2002**, *298*, 1759–1762. (c) Gerion, D.; Parak, W. J.; Williams, S. C.; Zanchet, D.; Mischeel, C. M.; Alivisatos, A. P. *J. Am. Chem. Soc.* **2002**, *124*, 7070–7074. (d) Wu, X.; Liu, H.; Liu, J.; Haley, K. N.; Treadway, J. A.; Larson, J. P.; Ge, N.; Peale, F.; Bruchez, P. *Nat. Biotechnol.* **2003**, *21*, 41–46. (e) Jaiswal, J. K.; Mattoussi, H.; Mauro, J. M.; Simon, S. M. *Nat. Biotechnol.* **2003**, *21*, 47–51.
- (6) For limited examples of saccharide-functionalized QDs, see: Chen, Y.; Ji, T.; Rosenzweig, Z. *Nano Lett.* **2003**, *3*, 581–584. For relevant gold nanoparticles, see: Barrientos, A. G.; de la Fuente, J. M.; Rojas, T. C.; Fernández, A.; Penadés, S. *Chem. Eur. J.* **2003**, *9*, 1909–1921.
- (7) (a) Murray, C. B.; Norris, D. J.; Bawendi, M. G. *J. Am. Chem. Soc.* **1993**, *115*, 8706–8715. (b) Qu, L.; Peng, X. *J. Am. Chem. Soc.* **2002**, *124*, 2049–2055.
- (8)  $\text{TOPOQD}$  prepared according to the literature method<sup>7b</sup> with a reaction time of 180 s had  $\lambda_{em} = 622$  nm (half-width = 24 nm) and a quantum yield of  $\Phi \cong 0.7$  ( $\lambda_{ex} = 500$  nm) in  $\text{CHCl}_3$ , as compared with respective literature values of 622 nm, 25 nm, and  $\sim 0.8$ .<sup>7b</sup>  $\text{TOPOQD}^{1b}$  in water had  $\lambda_{em} = 620$  nm (half-width = 23 nm) (Figure S2) and  $\Phi \cong 0.1$ .
- (9) Hayashida, O.; Mizuki, K.; Akagi, K.; Matsuo, A.; Kanamori, T.; Nakai, T.; Sando, S.; Aoyama, Y. *J. Am. Chem. Soc.* **2003**, *125*, 594–601.
- (10) For other examples of hydrophilization of  $\text{TOPOQD}$  upon hydrophobic associations, see refs 5b and 5e.
- (11) For the endocytic uptake of QD species, see refs 3b, 5d, and 5e.
- (12) Examples are adenovirus (70–90 nm), papovavirus (50 nm), parvovirus (20 nm), togavirus (50 nm), picornavirus (30 nm), hepatitis viruses (30–40 nm), HIV (100 nm), and low-density lipoprotein (LDL, 22 nm).

JA048792A